Nano Science & Nano Technology: An Indian Journal

Research | Vol 11 Iss 1

Statistically-Guided Optimization of the Catalysis of Cellulose Hydrolysis via Sulfamic Acid Functionalized Magnetic Iron/Iron(III) Oxide Core-Shell Nanoparticles

Ayomi SP[1*], Hongwang W[1], Asanka SY[1], Austin B[1], Jose C[1], Feng Xu[2], Donghai W[2], and Stefan HB[1]

[1]Department of Chemistry, Kansas State University, CBC Building 201, Manhattan, KS 66506, USA

[2] Kansas State University, Biological and Agricultural Engineering, Seaton Hall 150, Manhattan, KS 66506, USA

[*]**Corresponding author:** Ayomi SP, Department of Chemistry, Kansas State University, CBC Building 201, Manhattan, KS 665060401, USA, Tel: 17855326666; Fax: 17855326666; E-mail: ayomi.perera@ucl.ac.uk

Received: March 30, 2017; **Accepted:** May 03, 2017; **Published:** May 10, 2017

Abstract

Effective optimization of the degradation of cellulose into glucose, via a magnetic catalyst is achieved, for the first time, using statistically guided modification of reaction conditions. A highly efficient procedure for the large-scale synthesis of iron/iron(III) oxide (Fe/Fe_3O_4)

magnetic nanoparticles (MNPs), functionalized with sulfamic acid, has been developed. The acid functionalized MNPs have been used successfully, as a heterogeneous catalyst in the hydrolysis of cellulose to glucose and other yeast-convertible sugars, with a cellulose conversion of >50%. Optimization of the reaction conditions for the catalytic reactions has been accomplished, via the Doehlert matrix statistical approach. The Catalyst has been recovered up to 82% of its original weight, over 20 reaction cycles, with only marginal losses

of magnetic property and catalytic activity. Based on its' robustness and efficiency, we propose that the above catalyst is an excellent candidate for the industrial production of ethanol from plant cellulose.

Introduction

Magnetic nanoparticles consisting of iron oxide (Fe_2O_3, Fe_3O_4) or iron/iron(III) oxide (Fe/Fe_3O_4) have enormous potential in applications of a myriad of disciplines including catalysis [1-3], therapeutic biomedicine [4-6] and contrast-bio-imaging [7,8]. Consequently, various synthetic approaches for MNPs have been widely investigated, with extensive modifications that suit each specific application [9]. The magnetic property provides additional advantages of utilization including convenient separation, anchorage, and as a carrier medium [10-12]. In addition, MNPs can be used in combination with other materials such as zeolites for enhanced applications such as bio-catalysis [13,14].

Citation: Ayomi SP, Hongwang W, Asanka SY, et al. Statistically-Guided Optimization of the Catalysis of Cellulose Hydrolysis via Sulfamic Acid Functionalized Magnetic Iron/Iron(III) Oxide Core-Shell Nanoparticles. Nano Sci Nano Technol. 2017;11(1):115.

Magnetic core-shell nanoparticles have contributed to the advancement in the field of catalysis as novel bi-functional materials [15]. The shell carries a drug or functional group(s) that brings about catalysis, and/or anchors the particle to the substrate, and the magnetic core aids in separation, and in turn, the recycling of the catalyst [10,16]. Although the synthesis and functionalization of MNPs has progressed, enhancing their applicability tremendously, most synthetic techniques fail when attempted at larger scales [17]. This has greatly limited their use in industry and clinical applications [17]. We report an efficient procedure for the synthesis of acid functionalized MNPs that has been scaled up successfully, to obtain high material yields.

Cellulose is the most abundant natural organic polymer on earth and consequently, the largest source of biomass [18]. It is composed of long chains of D-glucose monomers, linked via β-1,4-glycosidic bonds. Cellulose can be hydrolyzed into its constituent glucose and other corresponding C6 and C5 sugars, via cleavage of the β-1,4-glycosidic bonds. The above process holds paramount significance in converting seemingly benign organic matter such as grass, wood waste and agricultural waste into industrially relevant materials such as ethanol, monomers of useful polymers and hydrocarbons [19,20]. Existing methods of cellulose degradation include the use of dilute mineral acids [21,22] supercritical water [23,24], ionic liquids [25,26], photo-conversion [27] and the use of enzymes [28,29]. These processes have significant challenges in separation, waste management, catalyst recovery, product yields, and the necessity of harsh and reaction conditions. Consequently, heterogeneous catalytic techniques have continuously evolved, as an attempt to address these drawbacks [30,31]. However, these processes have significant disadvantages in that they require flammable hydrogen gas and expensive noble metals, and the products have less applicability compared to glucose. Recently, research has shown that solid particles, functionalized with acid moieties, prove to be far more efficient catalysts for cellulose degradation [32].

The goal of this study was to develop a robust catalyst, with the potential to be used in an industrial scale, for production of ethanol via degradation of cellulose. We report, an effective scale-up synthesis of Fe/Fe_3O_4 core-shell MNPs, functionalized with sulfamic acid, as an efficient catalyst for the hydrolysis of cellulose into glucose. Reaction conditions for the above process have been optimized, for the first time, using the Doehlert matrix statistical approach. The results obtained provide valuable insight on how to enhance catalyst activity, in terms of product yield and selectivity as well as its reusability, in a systematic manner.

Experimental

All chemicals were purchased form Sigma-Aldrich and used without further purification.

Large scale synthesis of acid functionalized Fe/Fe_4O_3 MNPs

Synthesis of hexadecylamine hydrochloride HAD $_\times$ HCl: 30.05 g (0.1245 mol) of hexadecylamine (HDA) was combined with 650 ml of hexane and stirred vigorously under argon, until dissolved. Next, the flask was placed in an ice bath and 32 ml of HCl in 1,4-dioxane was added to the mixture (1:4 molar ratio of HDA:HCl) and stirred for 20 min. A white precipitate formed immediately, and was separated using vacuum filtration and dried under vacuum.

Synthesis of Fe/Fe_4O_3 MNPs: The synthetic approach used here is a slight variation of procedures reported in literature [1-3]. A mixture of 500 ml 1-octadecene (ODE), 7.0 g hexadecylamine hydrochloride (HAD × HCl) and 7.5 ml oleylamine was mechanically stirred (BODINE MOTOR, type NSP-11, # B0698049, 115V, 1350 RPM) at 120°C for 30 min, under argon. Next, the mixture was heated to 180°C and 25.0 ml of iron (0) pentacarbonyl ($Fe(CO)_5$) was added dropwise, while stirring, for 1 hour. Then the mixture was cooled to room temperature and the MNPs were allowed to precipitate out of solution. The supernatant was then removed and the nanoparticles were washed 5 times with 150 ml of hexane and ethanol each, respectively.

Coating of MNPs with silica and 3-amino-propyltrimethoxysilane (APTES): 600 ml of 2-propanol was added to the MNPs, followed by 30 min of mechanical stirring while sonicating via an ultra-sonic bath (Cole-Parmer ultrasonic cleaner). Next 75 ml of NH_4OH was added, followed by another 20 min of stirring and sonication. 15.0 ml of tetraethoxysilicate (TEOS) was added to 150 ml of 2-propanol and given dropwise to the above reaction mixture over 3 hours, with stirring and sonication. After the dropwise 5 addition, the mixture was reacted for an additional 3 hours. The nanoparticles were then collected with a magnet at the bottom of vessel and washed 5x with 150 ml ethanol and dried under vacuum and weighed. The nanoparticles were then dispersed in 600 ml of toluene and sonicated for 30 min, followed by refluxing at 110°C. 3.0 ml of 3-aminopropyl triethoxysilane (ATPES) was added to the above mixture and stirred and sonicated for 20 min. After completion of the reaction, the nanoparticles were collected and washed 5 times each, with 150 ml of toluene and methylene chloride, respectively.

Coating of silica-APTES coated MNPs with sulfamic acid: The nanoparticles were suspended in 150 ml of methylene chloride and chlorosulfonic acid (0.8 ml added for each 0.5 g of nanoparticles), and 50 ml of methylene chloride was added dropwise to the mixture over 20 min under argon. Finally, the nanoparticles were collected and washed 5 times with 150 ml of methylene chloride and dried under vacuum. An average weight of 12 g to 15 g of nanoparticles was collected for each synthetic batch (SCHEME 1).

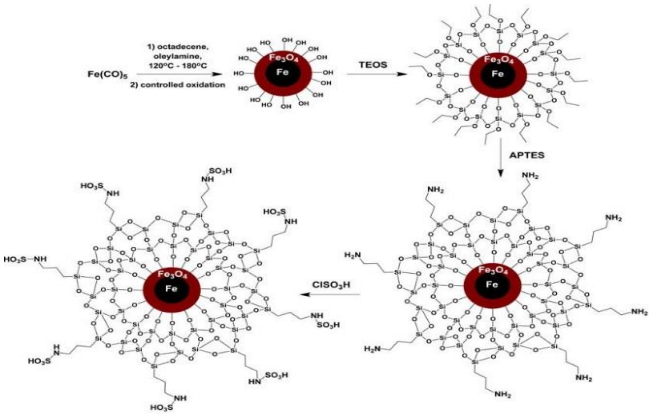

SCHEME 1. **(a) Synthesis procedure for the sulfamic acid functionalized, iron/iron(III) oxide magnetic nanoparticles. Note that both nanolayers that are formed upon addition of TEOS and APTES, are thicker than one layer.**

Characterization of non-functionalized and acid functionalized MNPs: Characterization of the non-functionalized and acid functionalized MNPs was carried out using TEM, SEM, EDX, XRD, FTIR, ICP and dynamic light scattering (DLS) and zeta potential measurements. The TEM samples were prepared by immersing carbon-coated 200-mesh copper grids into a solution of nanocatalysts, followed by washing the grids with dropwise chloroform and drying overnight in a desiccator. The dried grids were analyzed with a Philips CM 100 microscope operated at 100 kV. High-resolution TEM was recorded on FEI Tecnai F20XT, 200 kV; FEI, Hilsboro, OR. Powder X-ray diffraction (XRD) patterns were obtained on a Bruker D8 X-ray diffractometer with Cu Kα radiation. SEM images were taken using JEOL JSM-6480LV scanning electron microscope. EDX was performed using 7 the above instrument in low vacuum mode. ICP-OES experiments were carried out using a Varian 720-ES Inductively Coupled Emission Spectrometer [33]. The following wavelengths were utilized for quantitative element measurements: N: 174.272 nm; C: 247.856 nm; Si: 251.611 nm; S: 180.734; Fe: 259.940 nm. The quantitative analysis was based on calibration with element standards in 1N HNO3, with the exception of N, which consisted of HNO_3 in H_2O.

Determination of the number of -NH-SO_3H groups via titration: The amount of -NH-SO_3H groups loaded onto the MNP surface was determined as follows: 5.0 mg of MNPs from each batch were dispersed in 5.0 ml DI water and vortexed (Fisher Scientific Analog Vortex Mixer) for 5 min. Next, the mixtures were titrated with a 0.10 M NaOH solution. The initial pH of the MNP solution was 2.76, which is indicative of unreacted amine groups, which function as a buffer. Based on the titration volumes, the number of moles of NaOH, which correspond to moles of -NH-SO_3H, was calculated. The loading capacity was found to be 4.2×10^{-4} moles of sulfamic acid groups per 1.0 gram of MNPs, corresponding to 3.2% by weight (FIG. 1).

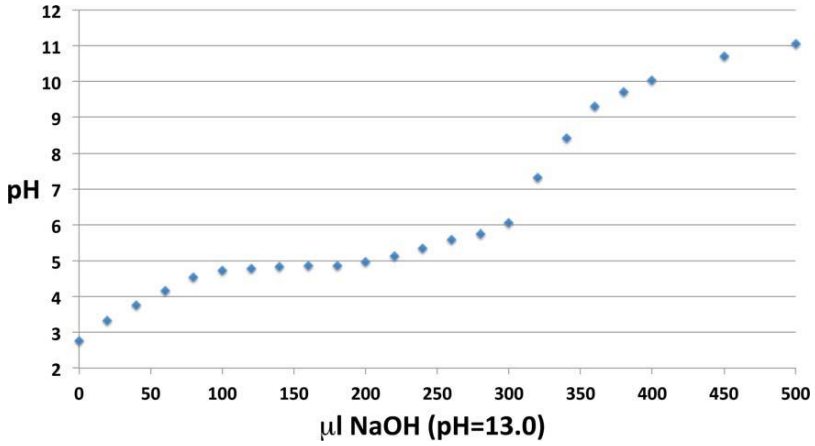

FIG. 1. **pH Titration of 5.0 mg MNP in 5.0 ml DI water. From this data, an apparent pKa=4.85 was determined.**

Cellulose degradation experiments: Commercial cellulose powder was purchased from Sigma Aldrich (microgranular). 0.25 g of cellulose powder was dispersed in 20.0 ml of distilled water and sonicated for 20 min. Next, the relevant amount of acid functionalized MNP catalyst was added to the mixture and sonicated for another 15 min. This mixture then reacted under high pressure in the Parr reactor (Parr Series 5500 High Pressure Compact Laboratory Reactor) at 1000 psi, at the relevant

temperature and time (initially 180°C and 1 hour respectively). Control experiments were conducted at 170°C and 1 h, at a starting pH of 2.76, excluding the MNP catalyst. The pH was adjusted by adding sulfuric acid.

Characterization of glucose and other cellulose degradation products: After the high-pressure reaction, MNPs were separated at the bottom of the vessel using a magnet and the supernatant was decanted. Next the collected solution was filtered through Millipore 0.45 μm syringe filters to remove the residual MNPs. The filtered solution was analyzed via HPLC (Shimadzu Prominence) and FTIR (Thermo Scientific NICOLET 380 FT-IR Spectrometer).

The amount of unreacted cellulose, after reaction was determined as follows: After reacting, the magnetic MNPs and a portion of adsorbed cellulose and other solids were separated using a 0.5 T permanent magnet. The supernatant was decanted off. The supernatant was then centrifuged at 10,000 rpm, at 5°C for 15 min., to remove any residual solids. The solid phases were combined and dried overnight in a drying oven at 70°C. The weight of the MNPs was deducted from the total solid weight to determine the remaining weight of cellulose. The MNPs were washed with hexane 50 mL per 1 mg of MNPs to remove all organic and polymeric residues (mostly 5-HMF and polymerized 5-HMF). The MNPs were stored for 24 h at 60°C prior to weighing. Sugar analysis was conducted using an HPLC 9 RCM-Ca^{2+} monosaccharide column (300 Å~7.8 mm; Phenomenex, Torrance, CA) with a refractive index detector. The HPLC was calibrated to external standards for sucrose, glucose, fructose, and maltose, using 80°C deionized water at a flow rate of 0.6 mL per minute. During HPLC analysis, samples were alternated with known standards to ensure accuracy of the measurements.

Doehlert matrix study on cellulose degradation conditions: In order to optimize the reaction conditions for cellulose degradation via acid functionalized MNPs, a Doehlert matrix study was conducted [34]. The latter is a statistical tool used in analytical sciences to experimentally determine optimum reaction conditions of a process. The model allows simultaneous changing of two or more reaction conditions, thereby significantly reducing the number of experiments necessary for an optimization study. We chose the simplest form of Doehlert matrix, which is characterized by the change of two reaction parameters; namely, catalyst percentage by cellulose weight and reaction temperature. Each matrix consists of a center point, which has known experimental conditions for the two chosen parameters. This point is probed in positive and negative directions, with an interval determined by the researcher. Next, each parameter is multiplied by a factor given in the model, generating a two-factor matrix. One such matrix consists of seven experiments in total, with a middle center point and six probe reactions, depicting the corners of a hexagon (TABLE 1). Conditions for the first matrix, designed for catalytic optimization are given in TABLE 1.

TABLE 1. **Conditions for Doehlert matrix 1 for cellulose degradation experiments.**

Experiment	Factor 1	Catalyst % by cellulose wt.	Calculated catalyst wt./mg	Factor 2	Temperature/°C
1	0	8	20	0	180
2	1	12	30	0	180

3	0.5	10	25	0.866	197
4	-1	4	10	0	180
5	-0.5	6	15	-0.866	163
6	0.5	10	25	-0.866	163
7	-0.5	6	15	0.866	197

After completion of the experiments in matrix 1, the parameters leading to the generation of the highest glucose concentration were determined via HPLC. Subsequently, matrices 2 and 3 were designed for further optimization of reaction conditions. Matrix 2 did not require conducting seven new experiments, but only three new experiments, which extended into a second matrix, in combination with four experiments from matrix 1 (TABLE 2).

TABLE 2. **Conditions for Doehlert matrix 2 for cellulose degradation experiments (Temperature taken to the closest integer value).**

Experiment	**Factor 1**	**Catalyst % by cellulose wt.**	**Calculated catalyst wt./mg**	**Factor 2**	**Temperature/°C**
5	0	6	15	0	163
6	1	10	25	0	163
1	0.5	8	20	0.866	180
8	-1	2	5	0	163
9	-0.5	4	10	-0.866	148
10	0.5	8	20	-0.866	148
4	-0.5	4	10	0.866	180

In matrix 3, the intervals for reaction parameters were adjusted to be smaller, in order to closely investigate the optimal conditions (TABLE 3).

TABLE 3. **Conditions for Doehlert matrix 3 for cellulose degradation experiments.**

Experiment	**Factor 1**	**Catalyst % by cellulose wt.**	**Calculated catalyst wt./mg**	**Factor 2**	**Temperature/°C**
11	0	4	15	0	170
12	1	6	25	0	170
13	0.5	5	20	0.866	179
14	-1	2	5	0	170
15	-0.5	3	10	-0.866	161
16	0.5	5	20	-0.866	161
17	-0.5	3	10	0.866	179

Further optimization experiments: A separate set of experiments were conducted at optimum temperature and catalyst % values (i.e. 170°C and 2% respectively), while the reaction being stopped each hour. The solid phase (MNP-cellulose-by product mixture) was separated out by centrifuging and the supernatant was replaced with distilled water, and pH adjusted to 2.76 via addition of HCl.

Results and Discussion

Acid functionalized iron/iron(III) oxide (Fe/Fe_4O_3) nanoparticles

In synthesizing magnetic Fe/Fe_4O_3 nanoparticles (MNP's), functionalized with sulfamic acid groups, we have taken into account lessons from earlier research on magnetic nanoparticle catalysts reported in the literature [35-38]. Most importantly, stable Fe cores under catalysis conditions reported here cannot be achieved without introducing an inner silica shell through controlled reaction of TEOS at Fe_3O_4. APTES alone does not lead to the formation of a tight shell around Fe/Fe_3O_4, leading to rapid corrosion in aqueous reaction environments. Scale-up production of these nanoparticles was successfully achieved in our laboratories to 12 g to 15 g per batch, resulting in 50 g in total. The MNPs were characterized using TEM (FIG. 2 and 3) and XRD (ESI FIG. S1) and DLS (ESI, FIG. S2 and S3) experiments. The pH 12 of the reaction mixture before and after the cellulose degradation reaction was 2.6 and 2.3, respectively

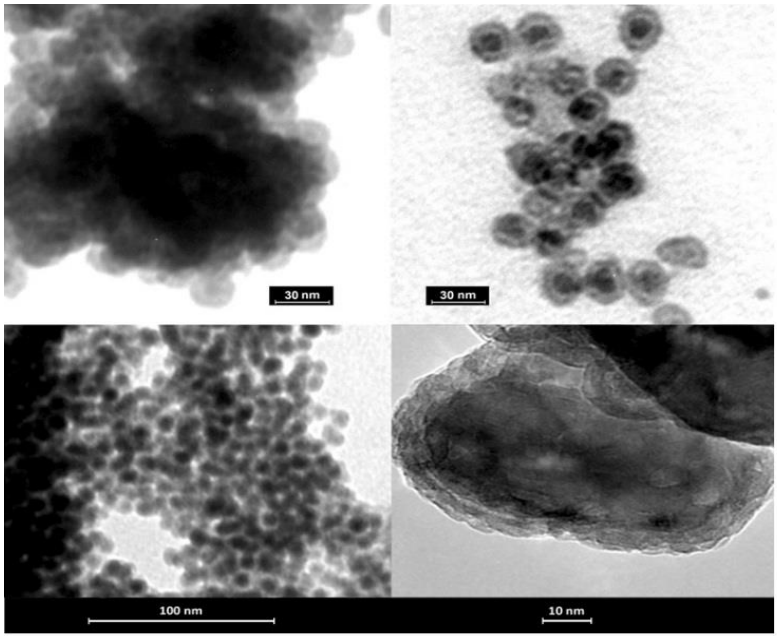

FIG. 2. **TEM images of MNPs. Top left and right: non-functionalized MNPs. Bottom left and right: acid functionalized MNPs**.

The elemental composition of the sulfamic acid functionalized magnetic Fe/Fe_3O_4-core/shell nanoparticles, as obtained from EDX and ICP-OES (ESI FIG. S4) is summarized in TABLE 4. Both the above methods yielded principally the same result.
It is noteworthy that the initial carbon and nitrogen content originates from APTES, as well as, potentially, hexadecylamine hydrochloride remaining on the surface. The latter is also responsible for the traces of chlorine found.

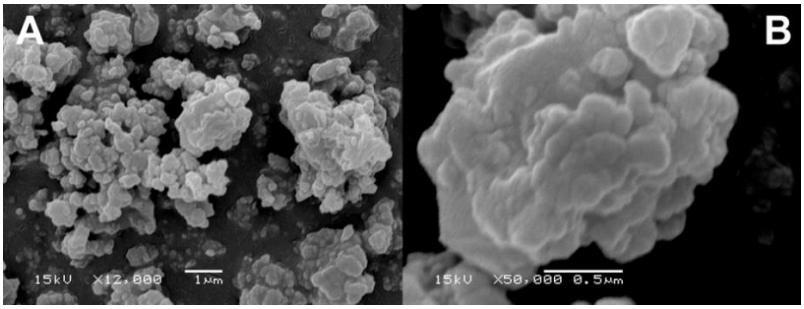

FIG. 3. **SEM images of MNP aggregates. A: x 12,000, B: x 50,000. The quasi-fractal nature of the aggregates is clearly discernible.**

TABLE 4. **Elementary composition of the sulfamic acid functionalized Fe/Fe_3O_4-core/shell nanoparticles in weight %.**

Method	C	N	O	Si	S	Cl	Fe
EDX	15.78	-	26.96	10.80	2.63	0.33	38.03
ICP-OES	15.43	6.37	-	11.73	2.64	-	37.14

Catalytic activity of the acid functionalized MNP particles

Catalytic reactions generated a mixture of sugars due to degradation of cellulose (ESI FIG. S5). The -NH-SO_3H moiety, on the functionalized MNPs is responsible for the hydrolysis of the glycosidic bonds in cellulose, resulting in generation of glucose monomers. However, glucose can easily isomerize into the 5-membered ring fructose and this in turn, can undergo dehydration to produce 5-hydroxymethylfurfural (5-HMF) (SCHEME 2).

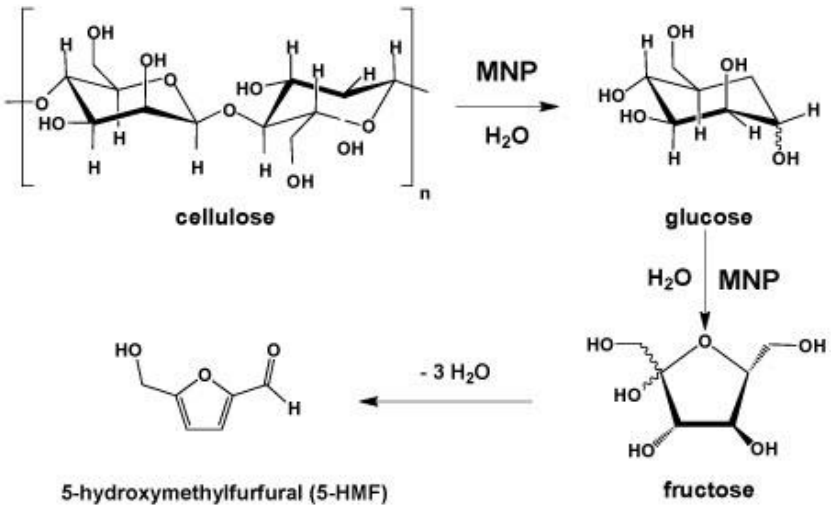

SCHEME 2**. Mechanistic paradigm for observed products in cellulose hydrolysis.**

The generation of 5-HMF is a highly undesirable feature in cellulose degradation, because it is toxic to ethanol producing

yeast. [39]. Apart from consumption of the major product glucose, this creates several other key disadvantages to the process. One issue is that it can undergo Diels-Alder reaction to form polymers, which can accumulate as solids in the reaction mixture, which disrupts separation of unreacted cellulose from products, stirring speed etc. (SCHEME 3).

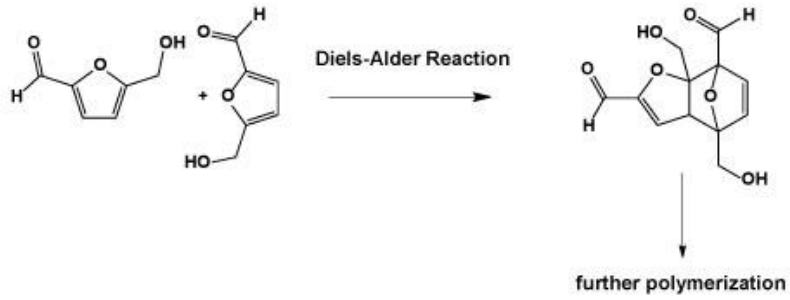

SCHEME 3. **Possible products from Diels-Alder reaction between 5-HMF molecules, and further reactions.**

As already mentioned, 5-HMF is toxic to yeast, which is commonly used in fermentation of glucose to produce ethanol. Therefore, feeding the products of cellulose degradation to the fermenting plant, including 5-HMF as a side product, often causes inefficiency in ethanol production. Hence, development of a catalyst that selectively catalyzes the reaction under conditions that minimize the production of 5-HMF, is highly desirable.

During our initial experiments, we observed the formation of glucose at a concentration of approximately 0.1 mg/ml and a number of other C6 and C5 sugars, along with dimers sucrose and maltose. It was evident that optimization of the reaction conditions was necessary in order to improve the glucose yield and selectivity. We have employed the Doehlert matrix as a statistical model, to investigate optimum reaction temperature and catalyst percentage by cellulose weight, for the cellulose hydrolysis reaction.

Optimization of reaction conditions for cellulose degradation via the Doehlert matrix

The first Doehlert matrix was designed to probe a temperature range of ± 20°C, at starting point of 180°C and a catalyst range of ± 4%, at a starting 8% point within Doehlert conditions (Experimental Section, TABLE 4, experiments 1-7, and FIG. 4). Since experiment #4 gave the highest glucose concentration, followed by #5 and #6, we explored lower reaction temperature conditions by conducting three other experiments, which resulted in matrix 2 (TABLE 4, experiments 8-10).

The lower temperatures did not seem to significantly increase the glucose content. Hence, a third matrix was designed, with relatively narrow temperature and catalyst probe limits (± 9°C and ± 2% respectively) to closely investigate the regions of conditions that give higher glucose concentrations. The amounts of 5-HMF formed are also included for comparison (TABLE 4, experiments 11-17).

TABLE 5. **Results of Doehlert matrices 1, 2 and 3.**

Experiment	Catalyst % by cellulose wt.	Temperature/°C	Glucose conc./mg/ml (± 0.01)	5-HMF conc./mg/ml (± 0.01)
1	8	180	0.35	0.20
2	12	180	0.32	0.18
3	10	197	0.22	-
4	4	180	0.38	0.23
5	6	163	0.37	0.44
6	10	163	0.34	0.46
7	6	197	0.34	0.03
8	2	163	0.35	0.26
9	4	148	0.01	0.11
10	8	163	0.25	0.17
11	4	170	0.25	0.33
12	6	170	0.10	0.26
13	5	179	0.17	0.20
14	2	170	0.34	0.42
15	3	161	0.09	0.35
16	5	161	0.10	0.28
17	3	179	0.28	0.19

Experiment #14 was identified as the optimal reaction condition point from matrix 3 and was used as the point of reference for further.

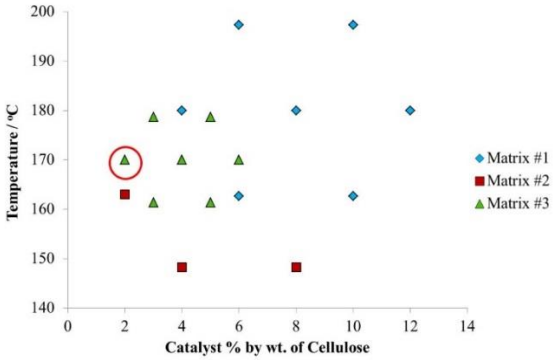

FIG. 4. **Investigation of optimum experimental conditions for cellulose degradation via Doehlert matrices. The red circle depicts the overall optimum point.**

Further optimization experiments

The matrices shed light onto optimum reaction conditions, governed by the change of reaction temperature and catalyst % by cellulose weight. However, the optimum point #14 generated a higher concentration of 5-HMF when compared to glucose. It is possible that other factors, such as reaction time, may play a key role in how much glucose can be collected before it is further converted to 5-HMF. To investigate the above, we conducted two other experiments using the same reactions conditions as experiment #14, but changing the reaction time from 1 hour to 3 and 5 hours respectively (experiments #18 and #19). It was evident that after 3 hours, the amount of glucose produced was significantly increased. However, at 5 hours it was far less, indicative of high degree of by-product formation. It is noteworthy that relatively lower catalyst amounts and temperatures produce higher concentrations of glucose.

TABLE 6. **Time dependent glucose optimization experiments.**

Experiment	**Catalyst % by cellulose wt.**	**Temperature/°C**	**Reaction time/hrs**	**Glucose content mg/ml (± 0.01)**	**5-HMF conc./mg/ml (± 0.01)**
18	2	170	3	0.62	0.11
19	2	170	5	0.18	0.10

In determining optimum reaction conditions, we also considered the conversion % of cellulose mass and the ratio between amounts of glucose and 5-HMF formed, during the reaction. Some key results are discussed below (TABLES 6 and 7).

TABLE 7. **Time dependent glucose optimization experiments: Key results.**

Experiment	**Glucose conc./mmolL^{-1}**	**5-HMF conc./mmolL^{-1}**	**Glucose: 5-HMF ratio**	**Conversion of cellulose mass/%**
4	2.11	1.82	1.2	27.12
8	1.94	2.06	0.9	18.96
14	1.89	3.33	0.6	19.04
18	3.44	0.87	4.0	24.4
19	1.00	0.79	1.3	29.2

It is evident from data depicted in TABLE 6 that when determining optimum conditions, the ratio of glucose to 5-HMF formed becomes a key factor. A higher glucose content alone or higher conversion of cellulose does not represent the overall

effectiveness of the process. Experiment #18 is clearly identified as the optimum point in terms of amount of glucose formed as well as glucose: 5-HMF ratio (See SI for details on experiments 1-20).

It is apparent that after the high-pressure reaction, the supernatant becomes concentrated with the reaction products and decomposition components from the acid functionalized MNPs. The pH change for the mixture, before and after reaction was 2.76 to 4.42. After the reaction, the MNPs were separated out by centrifuging and the supernatant appeared light brown in color. This layer is not magnetic hence the brown color is not due to presence of MNPs, but rather due to impurities from reactor/reaction mixture or dissolved Fe^{3+}. In contrast, the solid phase appeared highly magnetic.

We conducted a series of experiments where reactions were conducted at optimum temperature and catalyst % values, but the reaction was stopped each hour, the solid phase (MNP-cellulose-by product mixture) was separated out by centrifuging and the supernatant was replaced with distilled water, pH adjusted to 2.76 (TABLE 7). By replacing the solvent each hour. we remove the products and other unwanted impurities and prevent glucose produced from converting to 5-HMF. By adjusting the pH, we have recreated the protonation state of the sulfamic acid groups at the surface of the magnetic nanoparticle catalyst after synthesis (FIG. 1). Adjusting the starting pH to 2.76 significantly contributes to the observed increase in efficiency of cellulose hydrolysis and the observed maximum of glucose formation. It is noteworthy that carrying out the reaction at 170°C in an aqueous solution of pH 2.76 (starting) in the absence of the nanoparticle catalyst yielded a completely different distribution of products compared to the catalyzed reaction. The pH after 1h of reaction was above 5.5 in all cases. The main product formed under these conditions was 5-HMF, followed by 5-HMF oligomerization, as indicated in SCHEME 3. This finding clearly demonstrates why the use of sulfamic acid functionalized Fe/Fe_3O_4 core-shell nanoparticles are advantageous when producing sugars from cellulose.

TABLE 8. **Results of the 20 cycle catalytic study with solvent replacement every hour.**

Experiment	**Glucose conc./mgml^{-1}**	**5-HMF conc./mgml^{-1}**
20-1	0.00	0.32
20-2	0.34	0.38
20-3	0.42	0.25
20-4	0.23	0.10

20-5	0.17	0.06
20-6	0.24	0.05
20-7	0.16	0.04
20-8	0.18	0.00
20-9	0.14	0.00
20-10	0.38	0.00
20-11	0.26	0.00
20-12	0.10	0.00
20-13	0.04	0.00
20-14	0.08	0.00
20-15	0.04	0.00
20-16	0.04	0.00
20-17	0.03	0.00
20-18	0.00	0.00
20-19	0.00	0.00
20-20	0.00	0.00
Control	0.00	0.976

The above optimization experiments lead to the production of a significant concentration of glucose, up to 11 cycles. A higher concentration of 5-HMF is produced during the first 2 cycles, but this decreases rapidly up to cycle 7. There are no detectable amounts of 5-HMF formed after cycle 7. The total concentration of glucose formed after 20 cycles is 2.88 mg/ml and that of 5-HMF is 1.2 mg/ml. The control experiment (with MNPs) did not produce a significant amount of glucose (0.02 mg/ml), but generated a significant concentration of 5-HMF 0.17 mg/ml) (TABLES 8 and 9).

The total yield of glucose and 5-HMF obtained by weight, per weight of reacted cellulose was calculated. In comparison with yields from optimum points from matrices 1, 2 and 3, and extended optimization experiments, it is evident that replacing the solvent each hour gives far better yields for the major product glucose, while reducing the production of unwanted 5- HMF (FIG. 5).

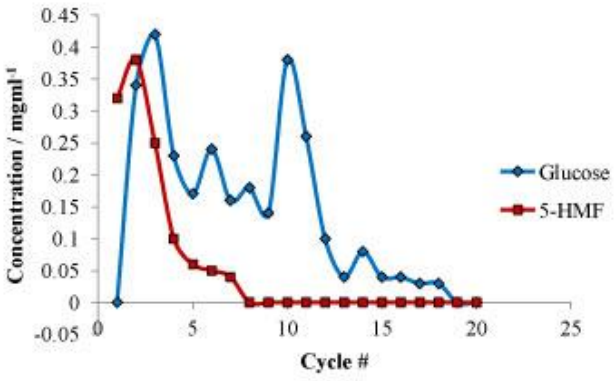

FIG. 5. **Concentrations of glucose and 5-HMF formed during 20-cycle study.**

TABLE 9. **Yield percentages of glucose and 5-HMF and total conversion of cellulose for key experiments.**

Experiment	Yield of glucose/%	Yield of 5-HMF/%	Conversion of cellulose mass/%
4	3.04	1.84	27.12
8	2.8	2.08	18.96
14	2.72	3.36	19.04
18	4.96	0.88	24.4
19	1.44	0.80	29.2
20 (All cycles)	23.04	9.6	>50

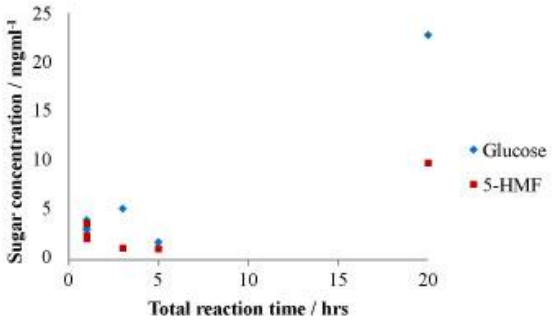

FIG. 6. **Concentrations of glucose and 5-HMF formed with reaction time.**

After 20 cycles with solvent replacement, more than 50% of cellulose mass was converted into sugars (ESI FIG. S6). The major product was glucose with 23.04% weight yield and 5-HMF was produced at a much lower 9.6% yield. The MNP

catalyst recovery after 20 cycles was 82%. The catalyst remained magnetic after 20 cycles, indicating that the Fe core is intact (FIG. 6). The high recovery and stability of the catalyst, together with high scalability in synthesis, makes it an excellent candidate for industrial applications. In particular, this method will be advantageous in ethanol production from plant matter, where 5-HMF levels need to be carefully controlled due toxicity to yeast, during fermentation.

We have successfully accomplished a scale-up synthesis procedure for efficient production of sulfamic acid functionalized iron/iron(III) oxide (Fe/Fe_3O_4) core-shell MNPs. The procedure allows synthesis of 12 g to 15 g of MNPs per reaction batch, and a total product yield of 50 g was achieved after 4 synthesis batches. The acid functionalized MNPs have been used as a heterogeneous catalyst for degradation of cellulose to predominantly glucose and other sugars with a >50% conversion of cellulose. The catalytic ability of the material has been optimized for the first time using the Doehlert matrix approach. Further optimization was carried out in order to enhance the glucose selectivity and yield. The catalyst appears to be quite robust, with 82% weight recovery, achieved over 20 reaction cycles with only marginal loss of magnetic property and catalytic activity. The above results depict a true possibility of utilizing the catalyst for the industrial scale production of ethanol via degradation of plant cellulose.

Acknowledgements

Financial support from the National Science Foundation (NSF EPS 0903806 and NSF ECCS 1128570) is gratefully acknowledged. The authors thank Prof. G. Hettiarachchi and Dr. Chammi Attanayake for performing the ICP-OES measurements.

REFERENCES

1. Giri S, Trewyn BG, Stellmaker MP, et al. Stimuli-responsive controlled- release delivery system based on mesoporous silica nanorods capped with magnetic nanoparticles. Angew Chem Int Edit. 2005;44(32):5038-44.
2. Wang H, Covarrubias J, Prock H, et al. Acid-functionalized magnetic nanoparticle as heterogeneous catalysts for biodiesel synthesis. J Phys Chem C. 2015;119(46):26020-8.
3. Wang H, Hodgson J, Shrestha TB, et al. Carbon dioxide hydrogenation to aromatic hydrocarbons by using an iron/iron oxide nanocatalyst. Beilstein J Nanotechnol. 2014;5:760-9.
4. Podaru G, Ogden S, Baxter A, et al. Pulsed magnetic field induced fast drug release from magneto liposomes via ultrasound generation. J Phy Chem B. 2014;118(40):11715-22.
5. Wang H, Shrestha TB, Basel MT, et al. Magnetic-Fe/Fe_3O_4-nanoparticle-bound SN38 as carboxylesterase-cleavable prodrug for the delivery to tumors within monocytes/macrophages. Beilstein J Nanotech. 2012;3:444-55.
6. Wang H, Shrestha TB, Basel MT, et al. Hexagonal magnetite nanoprisms: Preparation, characterization and cellular uptake. J Mat Chem B. 2015;3(23):4647-53.
7. Mahmoudi M, Simchi A, Imani M, et al. Optimal design and characterization of superparamagnetic iron oxide nanoparticles coated with polyvinyl alcohol for targeted delivery and imaging. J Phys Chem B. 2008:112(46):14470-14481.

8. Thomas LA, Dekker L, Kallumadil M, et al. Carboxylic acid-stabilized iron oxide nanoparticles for use in magnetic hyperthermia. J Mat Chem. 2009;19(36):6529-35.
9. Lu AH, Salabas EL, Schüth F. Magnetic nanoparticles: Synthesis, protection, functionalization, and application. Angew Chem Int Edit. 2007;46(8)1222-44.
10. Gu H, Xu K, Xu C, et al. Biofunctional magnetic nanoparticles for protein separation and pathogen detection. Chem Commun. 2006;9:941-9.
11. Safarik I, Safarıikova M. Use of magnetic techniques for the isolation of cells. J Chromatogr B. 1999;722(1-2):33-53.
12. Xu C, Xu K, Gu H, et al. Dopamine as a robust anchor to immobilize functional molecules on the iron oxide shell of magnetic nanoparticles. J Am Chem Soc. 2004;126(32):9938-9.
13. Lee J, Lee D, Oh E, et al. Preparation of a magnetically switchable bio-electrocatalytic system employing cross-linked enzyme aggregates in magnetic mesocellular carbon foam. Angewandte Chemie. 2005;117(45):7593-8.
14. Lu AH, Schmidt W, Matoussevitch N, et al. Nanoengineering of a magnetically separable hydrogenation catalyst. Angew Chem Int Edit. 2004;43(33):4303-6.
15. Mohapatra J, Nigam S, Gupta J, et al. Enhancement of magnetic heating efficiency in size controlled MFe2O4 (M=Mn, Fe, Co and Ni) nanoassemblies. RSC Adv. 2015;5(19):14311-21.
16. Park JI, Cheon J. Synthesis of “solid solution” and “core-shell” type cobalt: Platinum magnetic nanoparticles via transmetalation reactions. J Am Chem Soc. 2001;123(24):5743-6.
17. Hayden O. Grand challenges for translational materials science. Front Mat. 2014;1.
18. Klemm D, Heublein B, Fink HP, et al. Cellulose: Fascinating biopolymer and sustainable raw material. Angew Chem Int Edit. 2005;44(22):3358-93.
19. Chheda JN, Huber GW, Dumesic JA. Liquid-phase catalytic processing of biomass-derived oxygenated hydrocarbons to fuels and chemicals. Angew Chem Int Edit. 2007;46(38):7164-83.
20. Ragauskas AJ, Williams CK, Davison BH, et al. The path forward for biofuels and biomaterials. Science. 2006;311 (5760):484-9.
21. Mok WS, Antal MJ, Varhegyi G. Productive and parasitic pathways in dilute acid- catalyzed hydrolysis of cellulose. Ind Eng Chem Res. 1992;31(1):94-100.
22. Sherrard EC, Kressman FW. Review of processes in the united states prior to world war II. Ind Eng Chem. 1945;37(1):5-8.
23. Sasaki M, Adschiri T, Arai K. Kinetics of cellulose conversion at 25 MPa in sub- and supercritical water. AIChe J. 2004;50(1):192-202.
24. Sasaki M, Kabyemela B, Malaluan R, et al. Cellulose hydrolysis in subcritical and supercritical water. J Supercrit Fluid. 1998;13(1-3):261-8.
25. Nguyen TD, Nguyen HD, Nguyen PT, et al. Magnetic poly (Vinylsulfonic-co-Divinylbenzene) catalysts for direct conversion of cellulose into 5-hydroxymethylfurfural using ionic liquids. Mater Trans. 2015;56(9):1434-40.
26. Xiong Y, Zhang Z, Wang X, et al. Hydrolysis of cellulose in ionic liquids catalyzed by a magnetically-recoverable solid acid catalyst. Chem Eng J. 2014;235:349-55.
27. Wang L, Zhang Z, Zhang L, et al. Sustainable conversion of cellulosic biomass to chemicals under visible-light

irradiation. RSC Adv. 2015;5(104):85242-7.

28. Abushammala H, Hashaikeh R. Enzymatic hydrolysis of cellulose and the use of TiO_2 nanoparticles to open up the cellulose structure. Biomass Bioenerg. 2011;35(9):3970- 5.
29. Zhang YHP, Lynd LR. Toward an aggregated understanding of enzymatic hydrolysis of cellulose: Noncomplexed cellulase systems. Biotech Bioeng. 2004;88(7):797-824.
30. Fukuoka A, Dhepe PL. Catalytic conversion of cellulose into sugar alcohols. Angewandte Chemie. 2006;118(31):5285-7.
31. Luo C, Wang S, Liu H. Cellulose conversion into polyols catalyzed by reversibly formed acids and supported ruthenium clusters in hot water. Angewandte Chemie. 2007;119(40):7780-3.
32. Yamaguchi D, Kitano M, Suganuma S, et al. Hydrolysis of cellulose by a solid acid catalyst under optimal reaction conditions. J Phy Chem C. 2009;113(8):3181-8.
33. Schulz OWD. Analysing the elements Hydrocarbon Eng. 2008;3(11):102-6.
34. Ferreira SLC, Santos D, Quintella CM, et al. Doehlert matrix: A chemometric tool for analytical chemistry: Review. Talanta. 2004;63(4):1061-7.
35. Reziq AR, Alper H, Wang D, et al. Metal supported on dendronized magnetic nanoparticles: Highly selective hydroformylation catalysts. J Am Chem Soc. 2006;128(15):5279-82.
36. De Palma R, Peeters S,Van Bael MJ, et al. Silane ligand exchange to make hydrophobic superparamagnetic nanoparticles water-dispersible. Chem Mate. 2007;19(7):1821-31.
37. Kassaee MZ, Masrouri H, Movahedi F. Sulfamic acid-functionalized magnetic Fe_3O_4 nanoparticles as an efficient and reusable catalyst for one-pot synthesis of α-amino nitriles in water. Appl Catal A-Gen. 2011;395(1–2):28-33.
38. Peng S, Wang C, Xie J, et al. Synthesis and stabilization of monodisperse Fe nanoparticles. J Am Chem Soc. 2006;128(33):10676-7.
39. Nichols NN, Dien BS, Cotta MA. Fermentation of bioenergy crops into ethanol using biological abatement for removal of inhibitors. Bioresource Technol. 2010;101(19):7545-50.